Sugarcane bagasse fly ash as an attractive agro-industry source for VOC removal on porous carbon

Article *in* Industrial Crops and Products · August 2013

DOI: 10.1016/j.indcrop.2013.04.014

CITATIONS
34

READS
662

6 authors, including:

Gaurav Pande
Malvern Panalytical
5 PUBLICATIONS **82** CITATIONS
SEE PROFILE

Guy De Weireld
Université de Mons
108 PUBLICATIONS **7,512** CITATIONS
SEE PROFILE

Jean-François Lamonier
Lille University
144 PUBLICATIONS **5,309** CITATIONS
SEE PROFILE

Industrial Crops and Products 49 (2013) 108–116

Contents lists available at SciVerse ScienceDirect

Industrial Crops and Products

journal homepage: www.elsevier.com/locate/indcrop

Sugarcane bagasse fly ash as an attractive agro-industry source for VOC removal on porous carbon

Selvakumar Subramanian[a,b], Gaurav Pande[c], Guy De Weireld[d], Jean-Marc Giraudon[a,b], Jean-François Lamonier[a,b], Vidya S. Batra[c,*]

[a] Université Lille1 Sciences et Technologies, F-59655 Villeneuve d'Ascq, France
[b] CNRS UMR8181, Unité de Catalyse et Chimie du Solide – UCCS, France
[c] Centre for Energy and Environment, TERI University, 10 Institutional Area, Vasant Kunj, New Delhi 110070, India
[d] Thermodynamics Department, Faculté Polytechnique, UMons, Université de Mons, 20 Place du Parc, 7000 Mons, Belgium

ARTICLE INFO

Article history:
Received 4 April 2013
Accepted 12 April 2013

Keywords:
Sugarcane crop
Bagasse fly ash
Porous carbon
VOC removal
Adsorption

ABSTRACT

Sugarcane is an important industrial crop in India and the by-product bagasse is used as a fuel in sugar industries generating large quantities of fly ash. Unburned carbon from waste bagasse fly ash was used to prepare porous carbon for use as adsorbent and catalyst support for VOC removal. The carbons were prepared by steam activation and phosphoric acid modification. The textual properties, thermal stability and surface chemistry were characterized in detail using different techniques and the prepared samples from industrial unburned carbon were tested for toluene adsorption. A commercial carbon was also characterized and tested for comparison. The surface area and pore volume increased on activation while the surface oxygen was reduced. Phosphoric acid modification led to incorporation of phosphorus on the surface of the prepared carbons which led to improved thermal stability which was higher than the commercial activated carbon. The toluene adsorption capacity of the carbons synthesized in this study is improved with increasing degree of activation which corresponds with lower surface oxygen and greater micropore volume both of which promote VOC adsorption.

1. Introduction

Volatile organic compounds comprise a range of compounds including aromatics, alcohols and esters. These compounds are detrimental to both environment and health and as a result several options for their removal have been studied including adsorption (Jarraya et al., 2010; Romero-Anaya et al., 2010) and catalytic removal (Azalim et al., 2011; Quiroz-Torres et al., 2011, 2013; Wyrwalski et al., 2010). One such option for VOC removal is activated carbon which is commonly used as adsorbent, catalyst and catalyst support due to its unique properties. In addition to their stability and mechanical properties, they also have the ability to be tailored to obtain the required porosity and surface chemistry based on requirement (Juntgen, 1986). For use as catalytic supports for VOC oxidation, the hydrophobic nature of activated carbon supports prevents deactivation in the presence of moisture in the stream, compared to other hydrophilic supports (Bedia et al., 2010).

Several studies have examined the use of activated carbons as adsorbents. A study of benzene and toluene adsorption on different activated carbons has been done. It showed that the benzene adsorption was directly proportional to the narrow micropore volume which was obtained from CO_2 adsorption measurements. In the case of toluene, the adsorption depends on the narrow micropore volume (from CO_2 adsorption measurement) as well as the total volume of micropores from nitrogen adsorption measurements (Lillo-Rodenas et al., 2005). Reduction in surface oxygen by heat treating the samples also led to increase in adsorption capacity. A similar trend was observed for toluene adsorption on spherical activated carbon with high bed densities (Romero-Anaya et al., 2010). During adsorption of o-xylene as well it was found that adsorption increased with increase in surface area, total pore volume and reduction of surface oxygen (Li et al., 2011). Activated carbon prepared from durian shell using phosphoric acid treatment showed higher level of toluene adsorption with increase in phosphorus content which in turn led to increase in surface area (Tham et al., 2011). Carbon monoliths from petroleum pitch have shown adsorption of ethanol and benzene as a function of narrow micropore volume (Silvestre-Albero et al., 2010). As a catalyst support, wood charcoal was loaded with Co, Ni and Fe and tested for toluene oxidation. A high temperature heat treatment was required to promote partial graphitization and improve thermal stability. The best performance was obtained with cobalt catalyst (Kawada et al., 2011). Spent Pt–C catalyst has been regenerated with sulphuric acid treatment and used for BTX oxidation and showed better performance compared to untreated

* Corresponding author. Tel.: +91 11 24682100; fax: +91 11 24682144.
E-mail address: vidyasb@teri.res.in (V.S. Batra).

0926-6690/$ – see front matter © 2013 Elsevier B.V. All rights reserved.
http://dx.doi.org/10.1016/j.indcrop.2013.04.014

spent catalyst (Shim and Kim, 2010). Cobalt supported on different rice husk based carbon supports were tested for toluene oxidation and in some supports, carbon burn out occurred (Lu et al., 2009). Noble metal platinum supported on activated carbon showed high activity for benzene, toluene, xylene oxidation at low temperature compared to alumina support (Wu et al., 2000). The activity of tungsten oxide supported on activated carbon was more than other supports such as zeolite, silica, titania at lower temperatures; at higher temperatures, the stability of the support was a concern (Alvarez Morino et al., 2004). In a two cycle adsorption catalysis system o-xylene was adsorbed on Pd activated carbon catalyst at low temperature followed by increase in temperature for oxidation which was achieved at 140 °C for o-xylene (Huang et al., 2009). Activated carbon prepared with phosphoric acid method for thermal stability was used as a support for Pd and gave good activity for toluene and xylene (Bedia et al., 2010).

Thus it is seen that one of the challenges in using activated carbon as a catalyst or catalyst support is its lack of stability in oxidizing, high temperature environments. Several techniques have been examined to improve the stability of carbon (Stegenga et al., 1992). These include thermal treatment, acid treatment, addition of boron, phosphorus or silicon (Bedia et al., 2010; Lee and Radovic, 2003; Liu et al., 2010; Moene et al., 1996). Stegenga et al. (1992) found that a high temperature treatment led to better oxidation resistance as a result of reduction in active sites. The carbon impregnated with silica using tetraethoxy silane (TES) showed a marginal improvement in oxidation resistance. When the same samples were heated to obtain silicon carbide, the improvement was significant. Silicon carbide coated by chemical vapour deposition also led to improvement in oxidation resistance of activated carbon. The presence of surface phosphorus led to good oxidation resistance of phosphoric acid activated carbon. Similarly carbon cloth also exhibited good oxidation resistance on phosphorus impregnation.

Biomass is an attractive source for activated carbon and several studies have used a range of biomass and agro residue materials (Klasson et al., 2010; Zhong et al., 2012). Among them, bagasse has been explored for producing activated carbon by physical and chemical activation routes (Kalderis et al., 2008; Valix et al., 2004). Bagasse is normally used in the sugar industries as a fuel for cogeneration. The waste ash generated has a high amount of unburned carbon (20–33 wt%) (Umamaheshwaran and Batra, 2008). The unburned carbon (bagasse fly ash carbon) has the potential to be separated and activated.

Bagasse fly ash carbon has been characterized and examined for different applications (Batra et al., 2008). In this study the focus is on understanding the textural and surface properties of the activated and modified carbon obtained from sugarcane bagasse fly ash carbon. We have recently explored the use of some of these carbons as supports for VOC oxidation (Pande et al., 2012). The catalytic performance was strongly influenced by the thermal stability and low temperature adsorption of VOC by the supports. Therefore, in this paper, a detailed characterization of the supports is described. The carbons are being considered as both adsorbents to concentrate the VOC prior to catalytic oxidation as well as supports for transition metals for single step adsorption and catalytic oxidation. The carbon performances for industrial application depend on the adsorption capacities and the retainability, that is to say, the retention time of the COV under operating conditions without desorption. These two aspects are also studied in this work.

Table 1
Nomenclature of prepared samples.

Name	Description
SC	Separated carbon
CC	Commercial carbon
3AC	Separated carbon activated with 1:3 water ratio
5AC	Separated carbon activated with 1:5 water ratio
7AC	Separated carbon activated with 1:7 water ratio
P1	Separated carbon activated with 1:4 phosphoric acid ratio
P2	Separated carbon activated with 1:2 phosphoric acid ratio
P3	Separated carbon activated with 1:3 phosphoric acid ratio

2. Materials and methods

2.1. Sample preparation

Bagasse fly ash was obtained from a sugar mill in Northern India. The as received fly ash had an ash content of about 80 wt%. The carbon rich fraction was obtained by sieving to obtain a particle size of greater than 425 μm. This was further enriched by separating the fraction floating in water. This was dried and any remaining impurities like bagasse fibres were removed manually. This fraction is henceforth referred to as separated carbon and designated as SC.

The activated carbon was prepared by mixing the separated carbon with water in the required ratio and placing the mixture in a container with some air present. The air volume was kept fixed to see if it influenced the properties. This was then placed in another container and the gaps were filled with sand to obtain a near absence of air. The mixture was placed in a furnace at 550 °C and heated to 800 °C at a rate of 6 °C per minute. After 3 h at 800 °C, the sample was cooled in the furnace. The separated carbon – water ratios of 1:3, 1:5 and 1:7 were used and these are named 3AC, 5AC and 7AC respectively. The temperature and time were chosen based on initial trials and literature data (Liou, 2010).

Some samples were treated with phosphoric acid to improve the thermal properties. The phosphoric acid treatment was done using concentrated (85 wt%) phosphoric acid and carbon acid weight ratios of 1:2, 1:3 and 1:4. The mixture was dried at 110 °C for 24 h and activated at 900 °C in stainless steel tube reactor in flowing nitrogen at the rate of 0.1 SLPM. The temperature was increased from room temperature to 900 °C at the rate of 10 °C/min and then the temperature was maintained at 900 °C for 3 h and then allowed to cool in nitrogen flow. The sample prepared with 1:4 ratio had the least amount of phosphorus due to loss of phosphorus during activation as observed in the form of fumes from the reactor exit. Hence the samples 1:4, 1:2 and 1:3 are named P1, P2 and P3 respectively.

For comparison, commercial activated carbon (Merck, product no. 17505) with high surface area and thermal stability was also characterized. The nomenclature for all samples is shown in Table 1.

2.2. Characterization

The nitrogen adsorption was carried out at liquid nitrogen temperature (Micromeritics Tristar II 3020) on samples degassed at 150 °C for about 6 h under vacuum. The surface area was determined by the BET method. The micropore surface area and micropore volume were determined by *t*-plot and the total pore volume was determined by from single point total pore volume at P/P_o 0.97. X-ray diffraction studies were done with Bruker AXS D8 Advance diffractometer equipped with a copper anode (λ = 1.5406 Å). The 2-theta range was 10–80° for all the samples with a step-size of 0.02° and a hold time of 0.5 or 1 min. The diffraction patterns were indexed by comparison with the JCPDS files. The Raman spectra were recorded on a LabRAM Infinity spectrometer (Jobin Yvon) equipped with a liquid nitrogen detector and a frequency-double Nd:YAG laser supplying the excitation line at 532 nm. X-ray photoelectron spectra of the catalyst samples were recorded using a VG ESCALAB 220XL spectrometer equipped with an aluminium anode (Kα $h\nu$ = 1486.6 eV). The peak positions were corrected based on that of C 1s sp^2 peak which was taken as 284.6 eV. The spectra obtained were deconvoluted using

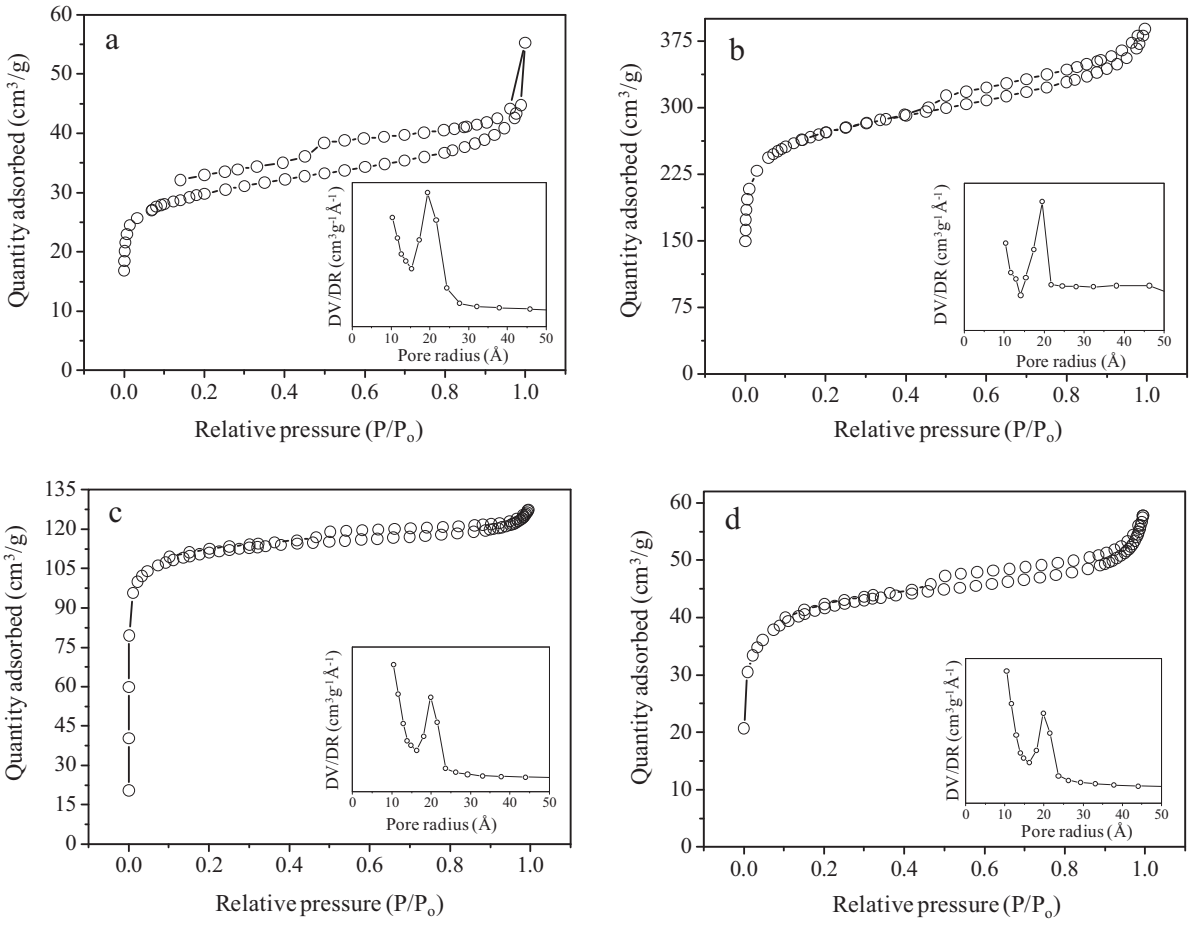

Fig. 1. N_2 isotherm and pore size distribution of (a) SC, (b) CC, (c) 7AC and (d) P3 samples.

curve-fitted with the nonlinear least-square iterative technique based on the Gaussian function after baseline subtraction using linear method. XPS quantification was performed by comparing the integrated peak areas with the appropriate relative sensitivity factors (RSFs). The FT-IR spectra were recorded from 400–4000 cm^{-1}, at room temperature, on a Nicolet 460 spectrophotometer. Samples were prepared by mixing 1 mg of powdered carbon materials with 100 mg of dried KBr. The samples were characterized for thermal stability using TGA-DTA (TA Instrument, SDT 2960) in 80% nitrogen, 20% oxygen atmosphere using a heating rate of 5 °C/min from ambient to 800 °C. The sample amount was around 5 mg and the flow rate was 100 mL/min.

2.3. Adsorption studies

The breakthrough study of toluene was carried out in a fixed bed reactor (internal diameter of 6 mm) containing 100 mg of carbon support. The outlet gas was analysed with the help of 7860A Agilent gas chromatograph equipped with a Flame Ionization Detector and CP-Wax 52 CB column. Prior to adsorption study the support was out-gassed in air flow (70 ml/min) from room temperature to 250 °C at the rate of 2 °C/min and maintained at higher temperature for about 4 h. The toluene adsorption was carried out at 28 ± 2 °C. The air flow used in these experiments was 100 ml/min, which contain 180 ppmv of toluene. Using these parameters, the breakthrough curves, which represent the concentration of VOC in the outlet gas versus time, are obtained. Adsorption capacity of the support was calculated by the numerical integration of the breakthrough curve. The other parameters such as breakpoint time, stoichiometric and saturation time were obtained by calculating the time at which the outlet toluene concentration was 5% ($t_{5\%}$), 50% ($t_{50\%}$) and 95% ($t_{95\%}$), respectively of the inlet toluene concentration. The length of unused bed (LUB) was calculated by using the formula shown below (Liu et al., 2011; Shiue et al., 2010).

$$\text{LUB} = \frac{t_{50\%} - t_{5\%}}{t_{50\%}} \times \text{bed length}$$

Adsorption isotherms of toluene were also measured at 303 K using a BELSORP-max automatic manometric sorption analyser (Bel Japan, Inc.) Prior to adsorption experiments, the samples (~50 mg) were outgassed under secondary vacuum (10^{-5} mbar) and heated at the rate of 1 °C/min to 150 °C and maintained at this temperature for 6 h. Prior to this, various tests carried out under an air flow at different temperatures showed similar outgassing mass sample at 250 °C. The adsorbents were placed in an adsorption chamber and the adsorbates were dosed. The pressure change was monitored and the adsorbed amount was calculated by a mass balance on the gas phase before and after adsorption when the equilibrium was reached (pressure variation lower than 0.1% for 1500 s). A typical adsorption experiment takes 5–10 days to obtain a complete toluene isotherm.

3. Results and discussions

3.1. Nitrogen adsorption

Fig. 1 shows the nitrogen adsorption isotherm and the pore size distribution for the separated carbon, commercial carbon, representative sample each of activated carbon (7AC) and phosphoric

Table 2
Textural properties of carbon samples.

Sample	BET surface area (m^2/g)	Micropore surface area (m^2/g)	Total pore volume (V_{total})[a] (cm^3/g)	$V_{micropore}/V_{total}$
SC	102.3	63.9	0.066	0.44
CC	933.9	582.1	0.567	0.47
3AC	428.0	297.7	0.196	0.53
5AC	489.0	363.2	0.227	0.58
7AC	430.4	309.4	0.197	0.56
P1	406.9	299.2	0.210	0.57
P2	465.6	302.5	0.223	0.47
P3	155.4	84.9	0.089	0.29

[a] From single point total pore volume at P/P_o 0.97.

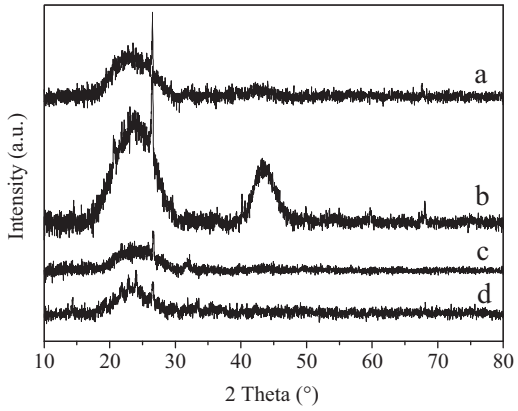

Fig. 2. X-ray diffraction pattern of: (a) SC, (b) CC, (c) 7AC and (d) P3.

acid modified carbon (P3). The textural properties of all samples are summarized in Table 2.

SC shows an initial increase in adsorption at low pressures followed by a relative flattening of the curve like a type I profile as per IUPAC classification (Sing, 1982) with a small hysteresis loop above a relative pressure value >0.4 indicating presence of micropores with some mesopores (Fig. 1a). The nitrogen adsorption increases with pressure in a continuous manner for the activated sample (7AC) like the type IV profile (Fig. 1c). This could be due to greater development of mesopores. A similar development of type IV profile after activation has been reported in case of activated carbon from bagasse (Liou, 2010). The adsorption isotherm of phosphoric acid modified carbon shows a small hysteresis loop indicative of micropores with small mesopores (Fig. 1d). The commercial carbon has higher nitrogen adsorption with type IV profile indicative of micro and mesopore presence (Fig. 1b). The pore size distribution from BJH analysis for activated carbon and phosphoric acid modified carbons shows that a high proportion of the pores radius close to the value of 20 Å.

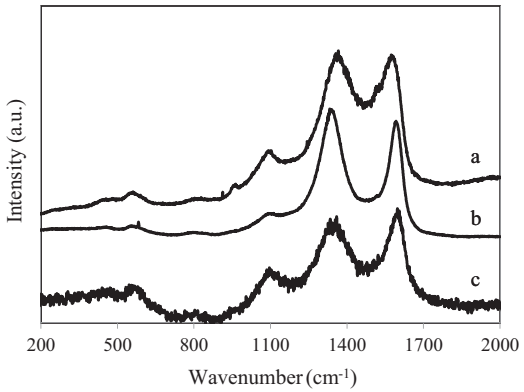

Fig. 3. Raman spectra of different carbon samples: (a) SC, (b) CC and (c) 7AC.

From Table 2 it is seen that the surface area of the activated carbon is higher than that of separated carbon and corresponds with carbon burn off as seen in higher residual weight after thermal analysis which will be discussed in a later section. Studies in literature have shown increase in surface area with increase in carbon burn off (Belhachemi and Addoun, 2011; Lu et al., 2010). The phosphoric acid modified samples show similar surface area for low P content samples (P1, P2) and a reduction in surface area at higher P content (P3). Studies on activated carbon from phosphoric acid treatment of different biomass sources have shown higher surface area compared to steam activation of the same biomass source after carbonization (El-Hendawy et al., 2008; Guo and Lu, 2003). In a lignocellulosic precursor, phosphoric acid causes bond cleavage and formation of crosslinks to form phosphate and polyphosphate bridges; the phosphate groups cause dilation in the structure which causes pores once the acid is removed (Bedia et al., 2010; Jagtoyen and Derbyshire, 1998). In this case, since the starting material is already carbonized, this influence is not observed. However, increasing the thermal cycling time in a bigger batch with slow cooling, led to higher surface area (Pande et al., 2012). The total pore volume of activated samples shows an increase compared to the separated carbon. The micropore volume to total pore volume ratio also shows an increase implying that the activation led to a greater increase in micropores than mesopores.

3.2. X-ray diffraction analysis

The room temperature XRD of separated carbon and commercial carbon is shown in Fig. 2. The commercial carbon shows broad peaks at 2θ values of around 24° and 44° which could be due to pores along graphite direction or graphite micro domains which have been observed in other activated carbons (Lazaro et al., 2007; Liou, 2010). In addition a sharp peak is seen superimposed on the broad peak which could be due to silica or graphite. Since commercial carbon has practically no ash (as will be discussed in later sections), it is assumed that the peak is due to graphite. A similar superimposition of graphite peak on a broad background

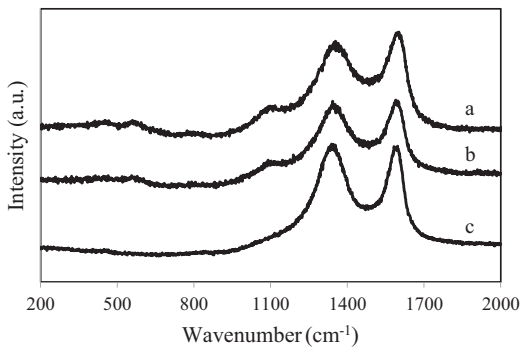

Fig. 4. Raman spectra of phosphoric acid modified activated carbon samples: (a) P1, (b) P2 and (c) P3.

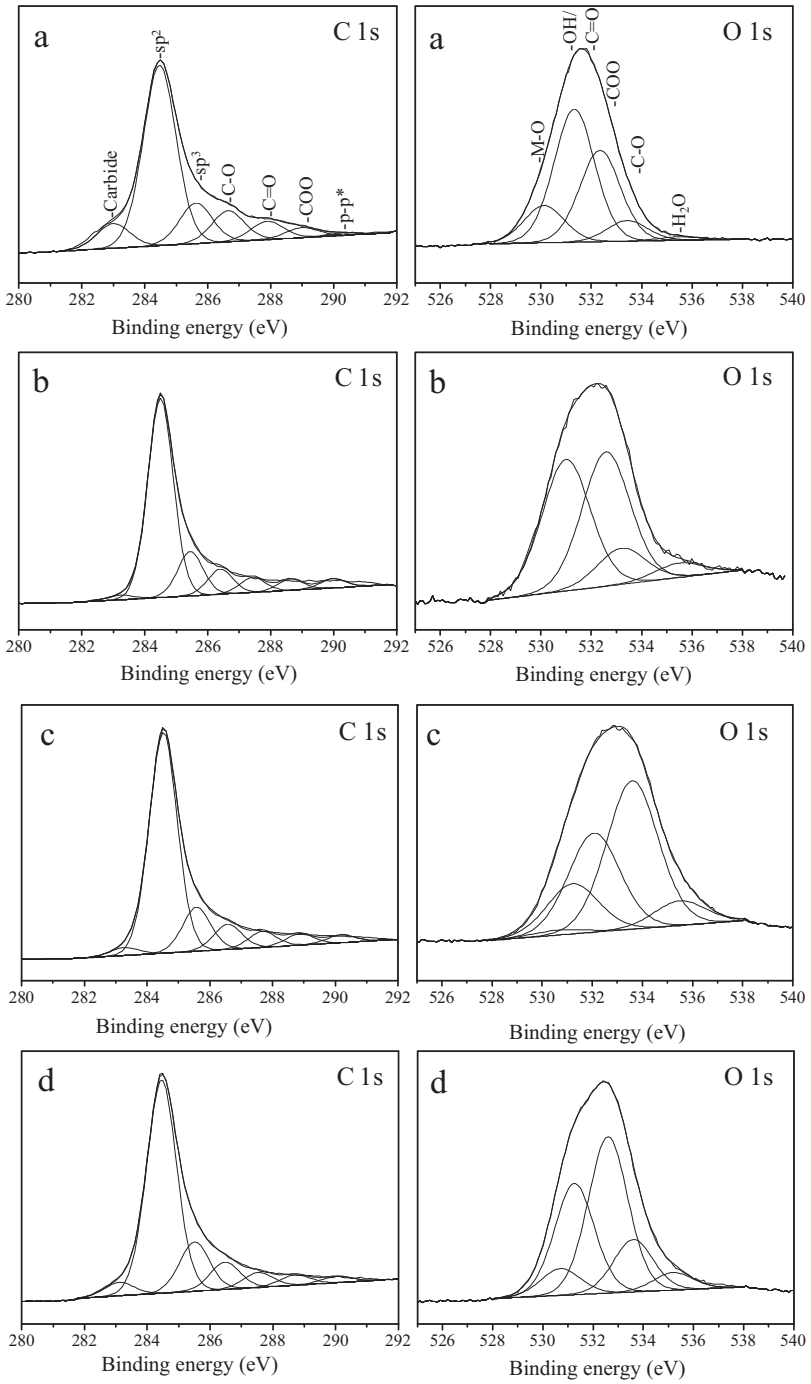

Fig. 5. Carbon and oxygen 1s XPS of (a) SC, (b) CC, (c) 7AC and (d) P3 samples.

peak has already been observed (Valix et al., 2008). The separated carbon however shows only the broad peak at 2θ of 24°. The pattern for 7AC is similar to that for SC but additional sharp peaks are observed which could be due to ash constituents which are more in the activated samples due to carbon burn off. In case of the phosphoric acid sample (P3), the broad carbon peaks are less obvious compared to separated and activated carbons. The samples also have additional peaks which appear to be from silicon and magnesium phosphates formed due to reaction with ash constituents. The other phosphoric acid samples (P1, P2) gave similar results.

3.3. Raman analysis

Fig. 3 shows the Raman spectra of separated carbon, commercial carbon and activated carbon (7AC). The samples show the characteristic D and G carbon peaks in the range of 1349–1358 cm^{-1} and 1597–1600 cm^{-1}, respectively. Pure graphite shows only G peak from in-plane vibrations with E_{2g} symmetry while amorphous carbon has an additional D peak induced by disorder from vibrations of sp^2 rings (Janes et al., 2007). Compared to separated carbon, it is observed that activated carbon has sharp well defined peaks. On activation, the D and G peaks are better defined compared to

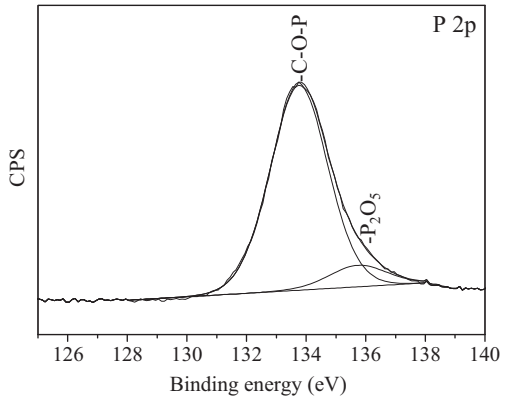

Fig. 6. Phosphorous 2p XPS of P3 sample.

separated carbon. A similar trend is seen on increasing phosphorus content as observed in Fig. 4. These indicate that with increasing extent of activation and increasing phosphorus content, the extent of short range order is increased. This has been observed while comparing activated and starting material as well as with increasing activation temperature (Janes et al., 2007; Lazaro et al., 2007).

3.4. XPS analysis

The deconvoluted peaks for carbon and oxygen are shown in Fig. 5. Seven carbon peaks are observed corresponding to carbide, sp^2, sp^3, C—O, C═O (carbonyl), COO (carboxyl) and π–π transition at binding energy regions of ~283, 284.5, ~285.4, ~286.4, ~287.4, ~288.6 and ~290 eV respectively. The oxygen could be deconvoluted to 4 or 5 peaks. In case of commercial carbon, no ash constituents were detected and the four oxygen peaks corresponding to OH/C═O, COO, C—OH/C—O—C and adsorbed water were obtained at binding energy regions of ~531, 532.6, 533.2 and 535.5 eV respectively. The separated carbon and all activated samples in addition showed a peak at ~530 eV corresponding to O—M where M could be Si, Ca from ash or phosphorus in case of phosphoric acid modified samples (Rosenthal et al., 2010). The phosphorus was present as C—O—P and some P_2O_5 at ~133.7 and 135.7 eV respectively (Fig. 6). Similar peaks have been obtained for phosphoric acid activated carbons from kraft lignin (Bedia et al., 2010).

The surface composition of the different samples is shown in Table 3. The carbon was primarily present as sp^2 and sp^3 carbon with a higher percentage of sp^2. The commercial carbon is primarily carbon with very less amounts of oxygen and no ash constituents could be detected on the surface. Separated carbon has a high level of both oxygen and ash constituents; however, the oxygen bonded to carbon is more than that present as mineral oxides from ash. Going from 3AC to 7AC, it is observed that the overall oxygen content is reduced and the reduction was found to be more from the C═O functional groups thereby showing an influence of the water carbon ratio. Lazaro et al. (2007) found a similar behaviour where the oxygen content in carbon reduced on activation of char and was reduced further at a higher activation temperature. This was accompanied by a substantial decrease in the C═O peak. The ash constituents of the activated carbon also show a decrease compared to separated carbon. During activation it is expected that the ash content would increase due to carbon burn off. While a higher ash content in activated samples is observed in thermal analysis, the surface composition does not show this trend.

The phosphoric acid modified carbon shows clearly that the surface phosphorus content of the prepared carbons increases from 1:2PAAC (P2) to 1:3PAAC (P3) but the higher phosphoric acid added in 1:4PAAC (P1) is not incorporated in the prepared carbon. These carbons also have a high oxygen content which is found to increase with increasing phosphorus content due to formation of C—O—P and P_2O_5 on the surface.

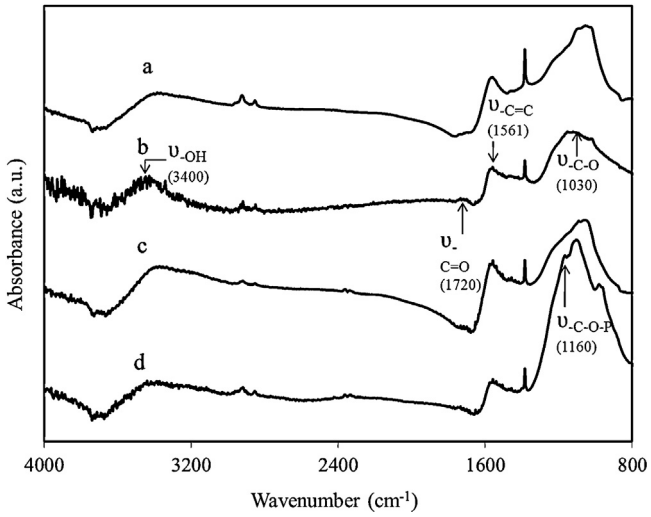

Fig. 7. FTIR spectra of carbon samples: (a) SC, (b) CC, (c) 7AC and (d) P3; the lines indicate key peak positions.

3.5. Infra red spectroscopy

The IR spectra of the carbons prepared from steam activation (7AC) and phosphoric acid modification (P3) of the fly ash based carbon are compared with the starting separated carbon and commercial carbon in Fig. 7. The starting carbon shows peaks corresponding to O—H group (around 3500 cm^{-1}), C═O group (around 1800 cm^{-1}), C═C bond (around 1500 cm^{-1} and 1400 cm^{-1}) and C—O (around 1000 cm^{-1}). On activation, the spectrum is similar. However, it is observed that the peak around 1800 cm^{-1} is less obvious. This is the same in case of the commercial carbon as well which does not show the C═O peak. This corresponds with the XPS data which shows reduction in C═O peak on activation and reduced oxygen content in activated carbon. During activation of another C═O containing precursor (pecan shells), the absorption band from C═O was found to shift from 1700 cm^{-1} to 1704 cm^{-1} and was attributed to change from carboxyl groups to ketones and aldehydes. The phosphoric acid modified sample has peaks at ~1150 cm^{-1} and 1000 cm^{-1} which could be from C—O—P and P—O respectively (Liou, 2010; Puziy et al., 2005).

3.6. Thermal analysis

The weight loss profile of commercial carbon, separated carbon, steam activated carbon (7AC) and phosphorus modified carbon (P3) is shown in Fig. 8. It can be seen that for the commercial carbon both the extent of weight loss and temperature of weight loss is higher indicating low ash content and good thermal stability. In comparison, the separated carbon has a low weight loss due to high ash content and a low oxidizing temperature. The steam activated sample show an increase in both ash content and oxidizing temperature. The samples prepared with other water–carbon ratios (3AC and 5AC) also showed similar behaviour. The onset of the combustion of the carbon is shifted to higher temperature and the ash content is higher. The thermal behaviour is related to the surface groups observed in XPS and FTIR analysis. The commercial carbon has low surface oxygen while the separated carbon has the highest oxygen content and also the lowest oxidation resistance. The

Table 3
Surface composition of samples from XPS analysis (at%).

	Carbon	Oxygen						Phosphorus	Ash constituents[a]
		O total	O as O—M (Si, Ca etc.)	OH/C=O	COO	C—O	Adsorbed water		
CC	94.75	5.26	0	2.19	2.23	0.60	0.24	0	0
SC	59.39	27.11	3.52	12.61	8.66	1.97	0.34	0.32	13.19
3AC	77.60	16.13	0.47	5.05	4.95	4.67	0.99	0	6.29
5AC	83.14	11.95	0.60	2.94	4.09	3.46	0.86	0.28	4.64
7AC	84.92	11.05	0.17	1.69	3.35	5.01	0.83	0.61	3.42
P1	76.73	14.33	0.57	3.69	4.97	3.65	1.45	7.56	1.4
P2	70.44	16.51	1.26	4.69	6.27	3.25	1.04	11.37	1.68
P3	64.73	19.40	1.43	5.92	8.33	2.79	0.93	14.35	1.54

[a] Si + Al + Ca + Mg + Na.

carbon on activation appears to lose the oxygen groups particularly the carbonyl group and shows improved thermal stability. A deterioration in thermal stability with incorporation of oxygen groups has been observed in a previous study. In inert atmosphere as well, incorporation of oxygen group by ozone treatment led to a lower temperature and greater extent of weight loss (Jaramillo et al., 2010). With increasing steam carbon ratio, the ash content increased as observed by increasing residual weight (not shown in figure). Rychlicki et al. (1999) have observed that HCl treatment of carbon led to improved thermal stability due to removal of metal cations that catalyse the carbon oxidation while subsequent treatment with HF to remove SiO_2 did not have a significant effect. Bagasse fly ash is comprised mainly of silica and hence it did not have a negative effect on the oxidation resistance.

The phosphoric acid modified carbon has an oxidation temperature even higher than that of commercial carbon. The other samples (P1, P2) also showed similar behaviour. The addition of phosphorus has shown to improve oxidation resistance of carbon by the formation of C—O—P, C—P and C—PO_3 bonds on the surface of the carbon. This has been used in C composites (Labruquere et al., 1998; Wu and Radovic, 2006) and activated carbon (Bedia et al., 2010; Labruquere et al., 1998).

3.7. Adsorption

Fig. 9 shows the breakthrough curve of all the prepared carbon supports. Commercial carbon reached saturation beyond 16 h (not shown in Fig) with a low breakpoint time ($t_{5\%}$) and a high saturation time ($t_{95\%}$) (Table 4). This sample also had a low bed height due to higher density and a low length of unused bed (LUB). The separated carbons and the activated and phosphorus modified carbons show a typical "S" shaped curve with small difference in adsorption time between $t_{5\%}$ and $t_{95\%}$. These carbons have a smaller LUB with SC having the lowest.

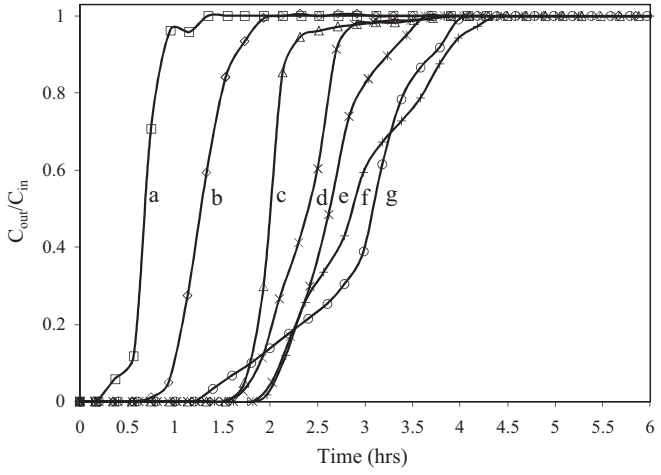

Fig. 9. Adsorption of toluene over different carbon samples: (a) P3, (b) P2, (c) SC, (d) P1, (e) 3AC, (f) 7AC and (g) 5AC. Inset shows the adsorption of commercial activated carbon samples (CC).

Fig. 10 shows the toluene adsorption isotherms for three samples (SC, 7AC, CC) at 303.15 K The SC isotherm shows an initial uptake at low pressure ($0.05 < P/P_o$) indicating the presence of micropores. First part of the isotherm is followed by a small increase of the curve corresponding to the presence of some mesopores. The 7AC isotherm increases continuously and significantly with pressure until 0.1 P/P_o due to the greater development of mesopores.

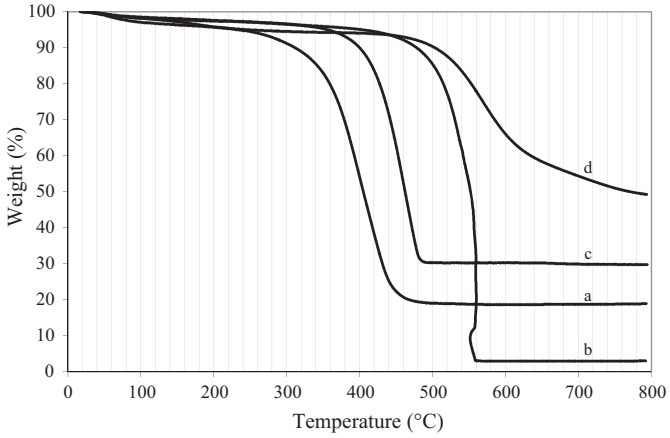

Fig. 8. Thermal analysis of carbon samples: (a) SC, (b) CC, (c) 7AC and (d) P3.

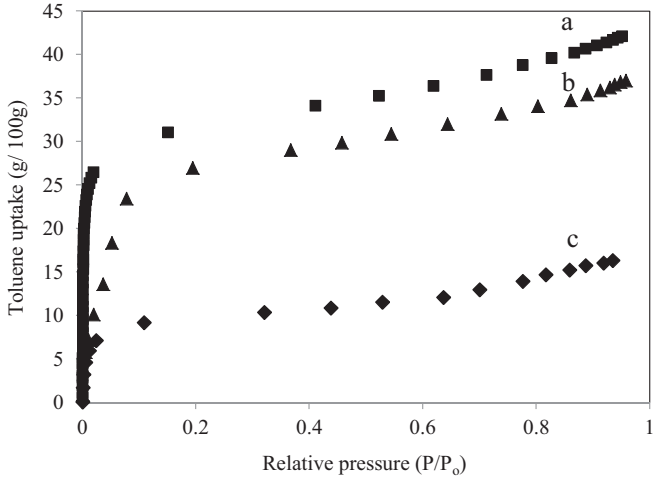

Fig. 10. Toluene adsorption isotherm over different carbon samples (a) CC, (b) 7AC and (c) SC.

Table 4
Breakthrough adsorption characteristics of different carbon samples.

Sample	BT[a] ($t_{5\%}$) (h)	SMT[b] ($t_{50\%}$) (h)	ST[c] ($t_{95\%}$) (h)	LUB[d] (cm)	SV[e] (min^{-1})	AC[f] (g/100 g sample)
CC	0.63	5.46	16.67	0.44	512.2	27.14
SC	1.73	2.00	2.37	0.11	301.0	8.17
3AC	2.00	3.42	2.62	0.33	322.1	10.32
5AC	1.49	3.08	3.88	0.41	272.4	11.47
7AC	2.02	2.87	3.98	0.24	297.2	11.52
P1	1.75	2.38	2.79	0.21	340.2	9.67
P2	0.93	1.27	1.77	0.16	386.8	4.99
P3	0.36	0.69	0.95	0.26	389.0	2.60

[a] Breakpoint time.
[b] Stoichiometric time.
[c] Saturation time.
[d] Length of unused bed.
[e] Space velocity.
[f] Adsorption capacity.

The commercial carbon (CC) presents a high toluene uptake at low pressure ($0.005 < P/P_o$), arising from strong interactions, confirming that activated carbon presents an important microporosity. For P/P_o from 0.005 to 0.9, adsorption occurs in the mesoporous spaces. For all sample, at high pressure ($P/P_o > 0.95$), capillary condensation occurs in the mesopores. The maximum adsorbed quantities of toluene at a relative pressure of 0.94 are 16.33, 36.20 and 41.68 g/(100 g of adsorbent) for SC, 7AC and CC respectively. These results are in relation with the specific surface area and pore volume of the adsorbents. The maximum uptake of material depends significantly on the adsorption capacity of the micropores,

The adsorption capacity for commercial carbon is higher (27 g of toluene/100 g of CC) than that of the other carbons which are in the range of 8–11 g/100 g of carbon except for P1 and P2 which had even lower adsorption capacity. Adsorption capacities ranging from 6 to 64 g/100 g have been reported for activated carbon in various studies as summarized by Lillo-Rodenas et al. (2005). The high adsorption capacity of CC may be due to high surface area and low surface oxygen groups (Table 3). On comparing the separated carbon and steam activated carbons, it is observed that the capacity is marginally improved with increasing water–carbon ratio which corresponds with lower surface oxygen and greater micropore volume both of which promote VOC adsorption (Lillo-Rodenas et al., 2005; Romero-Anaya et al., 2010). Presence of surface oxygen groups may prevent the direct aromatic π–π interaction between adsorbent and adsorbate and reduce the adsorption capacity. In the study of Lillo-Rodenas et al. (2005), good correlation was obtained between narrow micropore volume and adsorption capacity irrespective of carbon source and chemical treatment used. In the carbons of this study, the total pore volume and micropore volume did not show a linear trend when all samples were considered. However, when only steam activated samples and separated carbon were considered, the adsorption capacity showed a linear trend with micropore volume (Fig. 11). This indicates that the influence of phosphorus content was strong and led to reduction of adsorption capacity as observed in P2 and P3 samples.

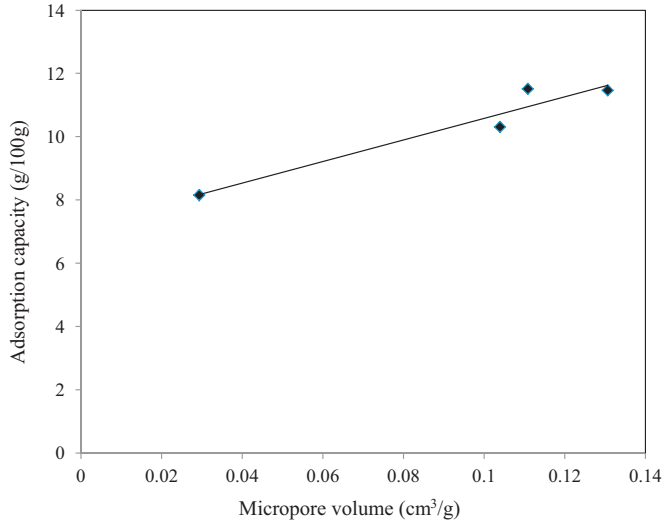

Fig. 11. Toluene adsorption capacity as a function of micropore volume for separated and steam activated carbons.

4. Conclusions

Steam activation of separated carbon from waste bagasse fly ash improves its surface area and total pore volume. The change in water to carbon ratio did not show much influence in the case of specific surface area but it influenced the surface composition considerably leading to lower surface oxygen groups with increasing water to carbon ratio and thereby improved thermal stability. The phosphoric acid modified carbons had better thermal stability than the commercial carbon due to presence of C—O—P groups. With higher phosphorus content, the surface area was reduced but the extent of order was improved as observed in Raman spectroscopy. The adsorption of toluene was higher with higher micropore volume, lower surface oxygen content and lower phosphorus content. Thus it is seen based on the preparation conditions, separated carbon from waste bagasse fly ash can be modified to obtain different surface areas and surface composition and a suitable balance between these properties is required to have both thermal stability and good adsorption. Good thermal stability is not only important for use as a catalyst support where the active phase can also influence the stability but also for desorption/regeneration after adsorption.

Acknowledgements

Support from Indo-French Centre for the Promotion of Advanced Research (IFCPAR)/Centre Franco-Indien pour la Promotion de La Recherche Avancée (CEFIPRA) is gratefully acknowledged.

References

Alvarez Morino, M., Ribiero, M.F., Silva, J.J.M., Carrasco-Marian, F., Maldonado-Hoadar, F.J., 2004. Activated carbon and tungsten oxide supported on activated carbon catalysts for toluene catalytic combustion. Environ. Sci. Technol. 38, 4664–4670.

Azalim, S., Franco, M., Brahmi, R., Giraudon, J.-M., Lamonier, J.-F., 2011. Removal of oxygenated volatile organic compounds by catalytic oxidation over Zr–Ce–Mn catalysts. J. Hazard. Mater. 188, 422–427.

Batra, V.S., Urbonaite, S., Svensson, G., 2008. Characterization of unburned carbon in bagasse fly ash. Fuel 87, 2972–2986.

Bedia, J., Rosas, J.M., Rodrıguez-Mirasol, J., Cordero, T., 2010. Pd supported on mesoporous activated carbons with high oxidation resistance as catalysts for toluene oxidation. Appl. Catal. B 94, 8–18.
Belhachemi, M., Addoun, F., 2011. Effect of Heat Treatment on the Surface Properties of Activated Carbons. E-J. Chem. 8, 992–999.
El-Hendawy, A.A., Alexander, A.J., Andrews, R.J., Forrest, G., 2008. Effects of activation schemes on porous, surface and thermal properties of activated carbons prepared from cotton stalks. J. Anal. Appl. Pyrolysis 82, 272–278.
Guo, J., Lu, A.C., 2003. Textural and chemical properties of adsorbent prepared from palm shell by phosphoric acid activation. Mater. Chem. Phys. 80, 114–119.
Huang, S., Zhang, C., He, H., 2009. In situ adsorption-catalysis system for the removal of o-xylene over an activated carbon supported Pd catalyst. J. Environ. Sci. 21, 985–990.
Jagtoyen, M., Derbyshire, F., 1998. Activated carbons from yellow poplar and white oak by H_3PO_4 activation. Carbon 36, 1085–1097.
Janes, A., Kurig, H., Lust, E., 2007. Characterisation of activated nanoporous carbon for supercapacitor electrode materials. Carbon 45, 1226–1233.
Jaramillo, J., Alvarez, P.M., Gomez-Serrano, V., 2010. Preparation and ozone-surface modification of activated carbon. Thermal stability of oxygen surface groups. Appl. Surf. Sci. 256, 5232–5236.
Jarraya, I., Fourmentin, S., Benzina, M., Bouaziz, S., 2010. VOC adsorption on raw and modified clay materials. Chem. Geol. 275, 1–8.
Juntgen, H., 1986. Activated carbon as catalyst support: a review of new research results. Fuel 65, 1436–1446.
Kalderis, D., Bethanis, S., Paraskeva, P., Diamadopoulos, E., 2008. Production of activated carbon from bagasse and rice husk by a single-stage chemical activation method at low retention times. Bioresour. Technol. 99, 6809–6816.
Kawada, S., Guo, Y., Jia, L., Chen, J., Kanehira, M., Kida, T., Tsuboyama, K., Kameyama, H., 2011. Catalytic oxidation of volatile organic compounds over Co-based catalysts supported on charcoal from thinned wood. J. Chem. Eng. Jpn. 44, 729–734.
Klasson, K.T., Ledbetter, C.A., Wartelle, L.H., Lingle, S.E., 2010. Feasibility of dibromochloropropane (DBCP) and trichloroethylene (TCE) adsorption onto activated carbons made from nut shells of different almond varieties. Ind. Crops Prod. 31, 261–265.
Labruquere, S., Pailler, P., Naslain, R., Desbat, B., 1998. Oxidation inhibition of carbon fibre preforms and C/C composites by H_3PO_4. J. Eur. Ceram. Soc. 18, 1953–1960.
Lazaro, M.J., Galvez, M.E., Artal, S., Palacios, J.M., Moliner, R., 2007. Preparation of steam-activated carbons as catalyst supports. J. Anal. Appl. Pyrolysis 78, 301–315.
Lee, Y.J., Radovic, L.R., 2003. Oxidation inhibition effects of phosphorus and boron in different carbon fabrics. Carbon 41, 1987–1997.
Li, L., Liu, S., Liu, J., 2011. Surface modification of coconut shell based activated carbon for the improvement of hydrophobic VOC removal. J. Hazard. Mater. 192, 683–690.
Lillo-Rodenas, M.A., Cazorla-Amoros, D., Linares-Solano, A., 2005. Behaviour of activated carbons with different pore size distributions and surface oxygen groups for benzene and toluene adsorption at low concentrations. Carbon 43, 1758–1767.
Liou, T.-H., 2010. Development of mesoporous structure and high adsorption capacity of biomass-based activated carbon by phosphoric acid and zinc chloride activation. Chem. Eng. J. 158, 129–142.
Liu, J., Yan, Y., Zhang, H., 2011. Adsorption dynamics of toluene in composite bed with microfibrous entrapped activated carbon. Chem. Eng. J. 173, 456–462.
Liu, Q.-S., Zheng, T., Wang, P., Guo, L., 2010. Preparation and characterization of activated carbon from bamboo by microwave-induced phosphoric acid activation. Ind. Crops Prod. 31, 233–238.
Lu, C.-Y., Wey, M.-Y., Chuang, K.-H., 2009. Catalytic treating of gas pollutants over cobalt catalyst supported on porous carbons derived from rice husk and carbon nanotube. Appl. Catal. B 90, 652–661.
Lu, L.Z., Maroto-Valer, M.M., Schobert, H.H., 2010. Catalytic effects of inorganic compounds on the development of surface areas of fly ash carbon during steam activation. Fuel 89, 3436–3441.
Moene, R., Boon, H.T., Schoonman, J., Makkee, M., Moulijn, J.A., 1996. Coating of activated carbon with silicon carbide by chemical vapour deposition. Carbon 34, 567–579.
Pande, G., Selvakumar, S., Batra, V.S., Gardoll, O., Lamonier, J.-F., 2012. Unburned carbon from bagasse fly ash as a support for a VOC oxidation catalyst. Catal. Today 190, 47–53.
Puziy, A.M., Poddubnaya, O.I., Martınez-Alonso, A., Suarez-Garcıa, F., Tascon, J.M.D., 2005. Surface chemistry of phosphorus-containing carbons of lignocellulosic origin. Carbon 43, 2857–2868.
Quiroz Torres, J., Giraudon, J.-M., Lamonier, J.-F., 2011. Formaldehyde total oxidation over mesoporous MnOx catalysts. Catal. Today 176, 277–280.
Quiroz-Torres, J., Royer, S., Bellat, J.-P., Giraudon, J.-M., Lamonier, J.-F., 2013. Formaldehyde: catalytic oxidation as a promising soft way of elimination. ChemSusChem 6, 578–592.
Romero-Anaya, A.J., Lillo-Ródenas, M.A., Linares-Solano, A., 2010. Spherical activated carbons for low concentration toluene adsorption. Carbon 48, 2625–2633.
Rosenthal, D.D., Ruta, M., Schlögl, R., Kiwi-Minsker, L., 2010. Combined XPS and TPD study of oxygen-functionalized carbon nanofibers grown on sintered metal fibers. Carbon 48, 1835–1843.
Rychlicki, G., Terzyk, A.P., Majchrzycki, W., 1999. The effect of commercial carbon de-ashing on its thermal stability and porosity. J. Chem. Technol. Biotechnol. 74, 329–336.
Shim, W.G., Kim, S.C., 2010. Heterogeneous adsorption and catalytic oxidation of benzene, toluene and xylene over spent and chemically regenerated platinum catalyst supported on activated carbon. Appl. Surf. Sci. 256, 5566–5571.
Shiue, A., Kang, Y.-H., Hu, S.-C., Jou, G.-T., Lin, C.-H., Hu, M.-C., Lin, S.-I., 2010. Vapor adsorption characteristics of toluene in an activated carbon adsorbent-loaded nonwoven fabric media for chemical filters applied to cleanrooms. Build. Environ. 45, 2123–2131.
Silvestre-Albero, A., Ramos-Fernandez, J.M., Martınez-Escandell, M., Sepulveda-Escribano, A., Silvestre-Albero, J., Rodrıguez-Reinoso, F., 2010. High saturation capacity of activated carbons prepared from mesophase pitch in the removal of volatile organic compounds. Carbon 48, 548–556.
Sing, K.K.S.W., 1982. Reporting physisorption data for gas/solid systems with special reference to the determination of surface area and porosity (provisional). Pure Appl. Chem. 54, 2201–2218.
Stegenga, S., Van Waveren, M., Kapteijn, F., Moulijn, J.A., 1992. Stability of carbon-supported catalysts in an oxidizing environment. Carbon 30, 577–585.
Tham, Y.J., Latif, P.A., Abdullah, A.M., Shamala-Devi, A., Taufiq-Yap, Y.H., 2011. Performances of toluene removal by activated carbon derived from durian shell. Bioresour. Technol. 102, 724–728.
Umamaheshwaran, K., Batra, V.S., 2008. Physico-chemical characterisation of Indian biomass ashes. Fuel 87, 628–638.
Valix, M., Cheung, W.H., McKay, G., 2004. Preparation of activated carbon using low temperature carbonisation and physical activation of high ash raw bagasse for acid dye adsorption. Chemosphere 56, 493–501.
Valix, M., Cheung, W.H., Zhang, K., 2008. Role of chemical pre-treatment in the development of super-high surface areas and heteroatom fixation in activated carbons prepared from bagasse. Microporous Mesoporous Mater. 116, 513–523.
Wu, J.C.-S., Lin, Z.-A., Tsai, F.-M., Pan, J.-W., 2000. Low-temperature complete oxidation of BTX on Pt/activated carbon catalysts. Catal. Today 63, 419–426.
Wu, X.X., Radovic, L.R., 2006. Inhibition of catalytic oxidation of carbon/carbon composites by phosphorus. Carbon 44, 141–151.
Wyrwalski, F., Giraudon, J.-M., Lamonier, J.-F., 2010. Synergistic coupling of the redox properties of supports and cobalt oxide Co_3O_4 for the complete oxidation of volatile organic compounds. Catal. Lett. 137, 141–149.
Zhong, Z.-Y., Yang, Q., Li, X.-M., Luo, K., Liu, Y., Zeng, G.-M., 2012. Preparation of peanut hull-based activated carbon by microwave-induced phosphoric acid activation and its application in Remazol Brilliant Blue R adsorption. Ind. Crops Prod. 37, 178–185.